Maximized performance of dye solar cells on plastic: a combined theoretical and experimental optimization approach

Yuelong Li,[a,b,†] *Sol Carretero-Palacios,*[a,†] *Kicheon Yoo,*[b,c,†] *Jong Hak Kim,*[c] *Alberto Jiménez-Solano,*[a] *Chul-Ho Lee,*[d] *Hernán Míguez*[a] *and Min Jae Ko*[b,d,e]

[a]Multifunctional Optical Materials Group, Instituto de Ciencia de Materiales de Sevilla, Consejo Superior de Investigaciones Científicas−Universidad de Sevilla (US-CSIC), Américo Vespucio 49, 41092 Sevilla, Spain.

[b]Photo-Electronic Hybrids Research Center, Korea Institute of Science and Technology, Seoul 02792, Republic of Korea

[c]Department of Chemical and Biomolecular Engineering, Yonsei University, Seoul 03722, Republic of Korea

[d]KU-KIST Graduate School of Converging Science and Technology, Korea University, Seoul 02841, Republic of Korea

[e]Green School, Korea University, 145, Anam-ro, Seongbuk-gu, Seoul 02841, Republic of Korea.

[†] These authors contributed equally to this work. Correspondence and requests for materials should be addressed to H.M. and M.J.K (email: h.miguez@csic.es and mjko@kist.re.kr).

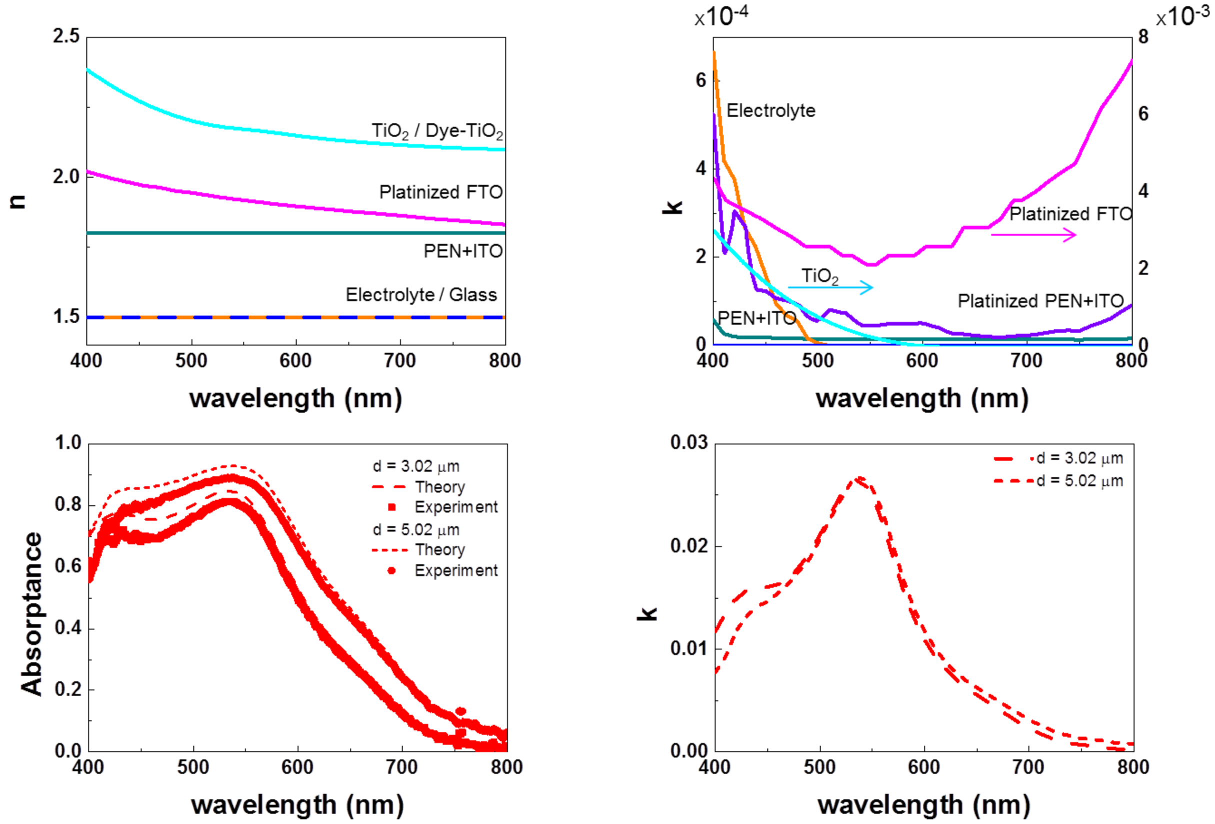

Figure S1. Top panels: Complex refractive index $\tilde{n}_m(\lambda) = n_m(\lambda) + ik_m(\lambda)$ of all materials considered in the theoretical evaluations. It is assumed that $n_{PEN+ITO}(\lambda) = n_{Platinized\ PEN+ITO}(\lambda)$. Bottom panels: optical characterization of simple Glass-FTO-Electrode samples. The thicknesses of the electrodes are 3.02 and 5.02 microns, and they are made of a 50% porous titania matrix containing 'nanoglue' and infiltrated with dye molecules. Left panel displays experimental and calculated absorptance, using the extracted complex refractive index (applying the formalisms described in Refs [1,2,3]) shown on the right panel. For saturated thicker electrodes employed in DSC in this work, it is assumed that $k_{Dye}^{Satur}(\lambda) = 1.5 \cdot k_{Dye}(\lambda)$.

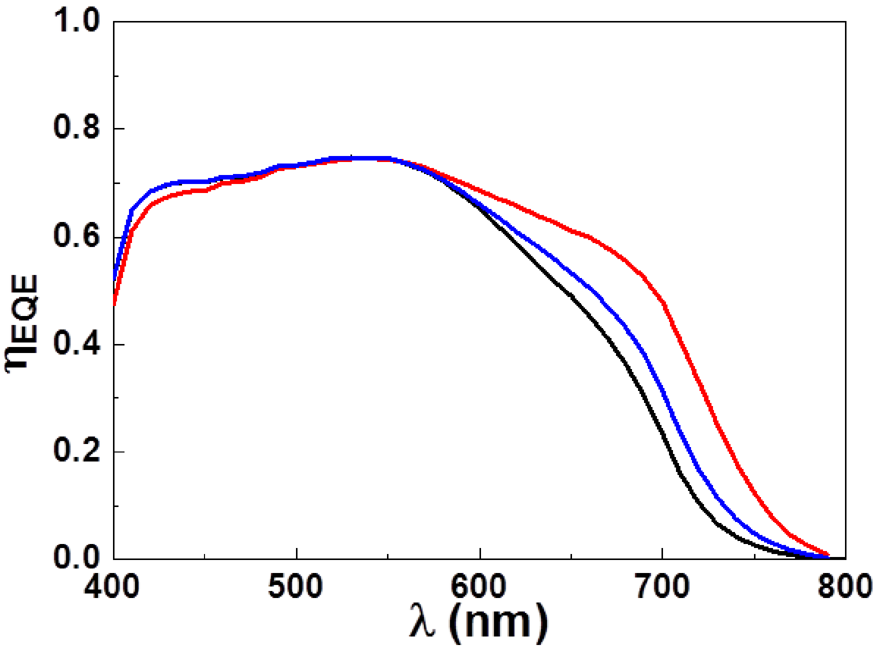

Figure S2. Theoretical calculations of the $\eta_{EQE}(\lambda)$ of a plastic cell. Black curve corresponds to a 8.55 microns electrode without scatterers, red one to a 8.65 microns electrode with 30% of nanoparticles of radius 160 nm, and blue one to a 8.55 microns electrode with a scattering layer of 4 microns. The effective electron diffusion length is taken to be $L_e = 8$ microns.

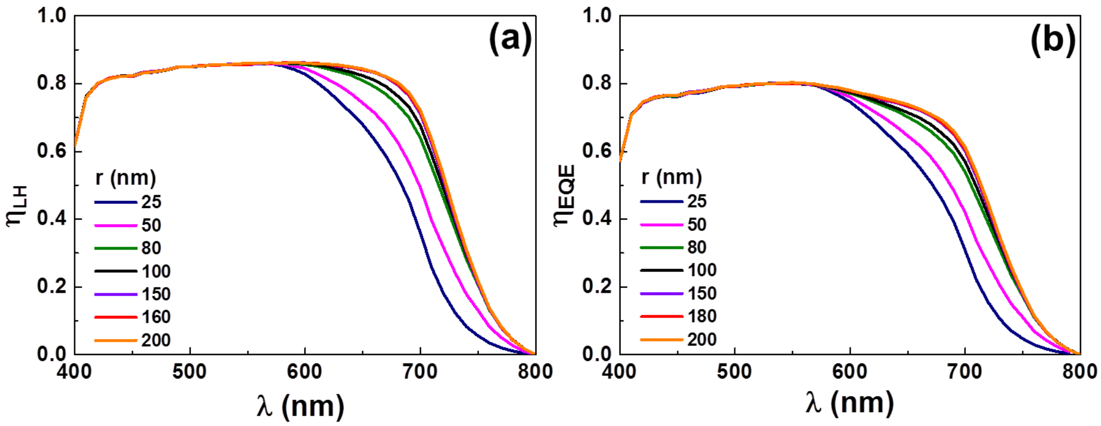

Figure S3. (a) Theoretical calculations of $\eta_{LH}(\lambda)$ (or absorptance) of plastic cells consisting on a 11.3 microns electrode containing scatterers of different radius (25, 50, 80, 100, 150, 160 and 200 nm, as indicate in the labels). The electrode consists of a first 2.8 microns layer without scatterers, and a second layer on top of 8.5 microns with 30% of scatterers. (b) Corresponding calculations of the $\eta_{EQE}(\lambda)$ spectra taking $L_e = 16$ microns.

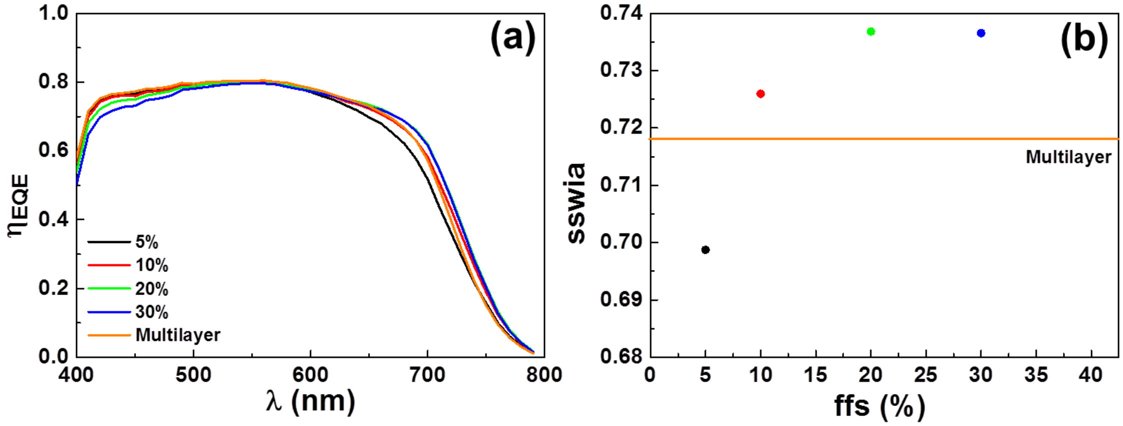

Figure S4. (a) Theoretical calculations of the $\eta_{EQE}(\lambda)$ of a plastic cell with a 12.5 micron electrode containing scatterers. The electrode consists of a first 3.125 microns layer without scatterers, and a second layer on top with scatterers of radius 160 nm at different concentrations (ff_s = 5%, 10%, 20% and 30%, as indicated in the labels). Results are compared with a multilayer configuration in which the first layer does not contain scatterers and the concentration of the 3 consecutive layers on top (of 3.125um each one) is increased: 10%, 20% and 30%. The electron diffusion length is taken to be $L_e = 16$ microns. (b) Corresponding sswia values. The solar spectrum weighted integrated absorption (η_{sswia}) is defined by $\eta_{sswia} = \frac{\int_{400}^{800} \eta_{LH}(\lambda) \cdot \text{AM1.5} d\lambda}{\int_{400}^{800} \text{AM1.5} d\lambda}$, with AM1.5 the normalized solar spectrum at the Earth surface.

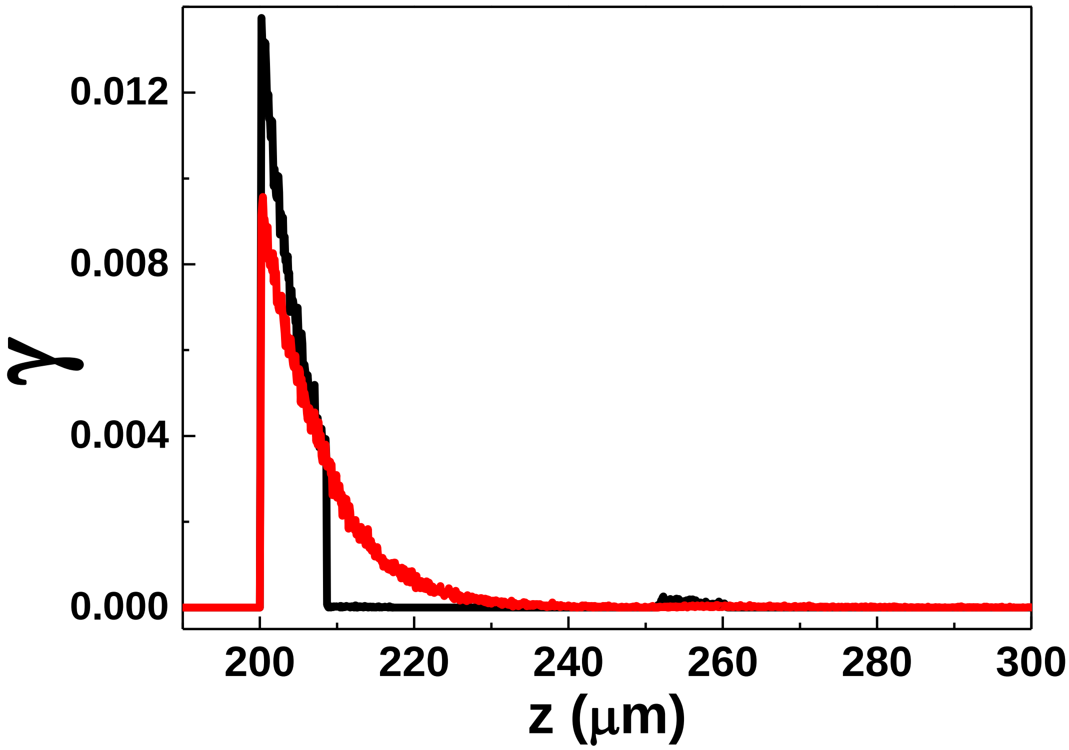

Figure S5. Theoretical calculations of the optical path (z) covered by absorbed photons by dye molecules normalized to the total number of photons (γ) injected at λ = 650 nm in rigid cells without light scatterers (black curve) or including 30% of TiO_2 scatterers with r = 160 nm. The cell consists on a PEN and ITO substrate (200 microns thickness), an 8.5 microns electrode, followed by an electrolyte of 21.5 microns, and followed by platinized FTO and glass counter electrode.

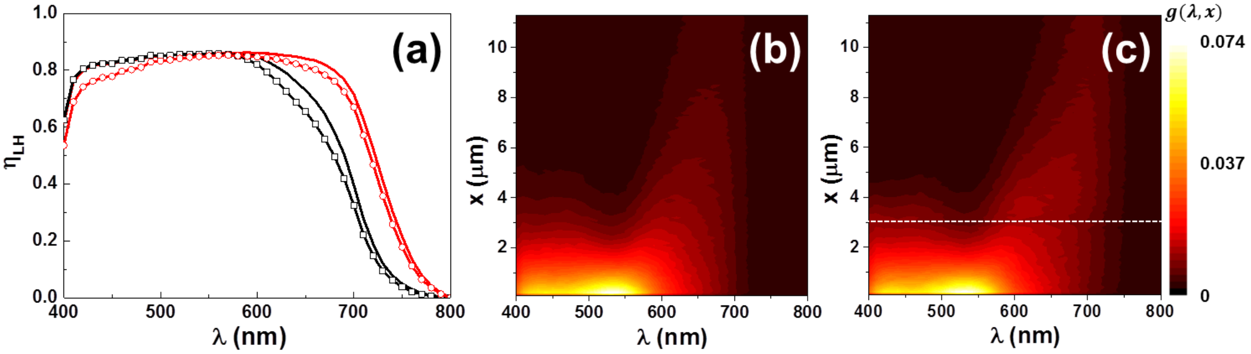

Figure S6. (a) Theoretical calculations of $\eta_{LH}(\lambda)$ (or absorptance) of a plastic cell with a total thickness of 11.3 microns. Black solid curve corresponds to an electrode without scatterers, and red solid curve to an electrode consisting on a first 2.8 micron layer without scatterers, and a second layer con top of 8.5 micron with 30% of scatterers (r = 160 nm). For comparison, empty symbols account for the absorptance of an 8.55 micron electrode without scatterers (black circles), and a 8.65 micron electrode with 30% scatterers (r = 160 nm, red circles). (b) and (c) absorption profiles as a function of the wavelength for each 11.3 micron electrode, (b) without scatterers and (c) with 30% scatterers (r = 160 nm).

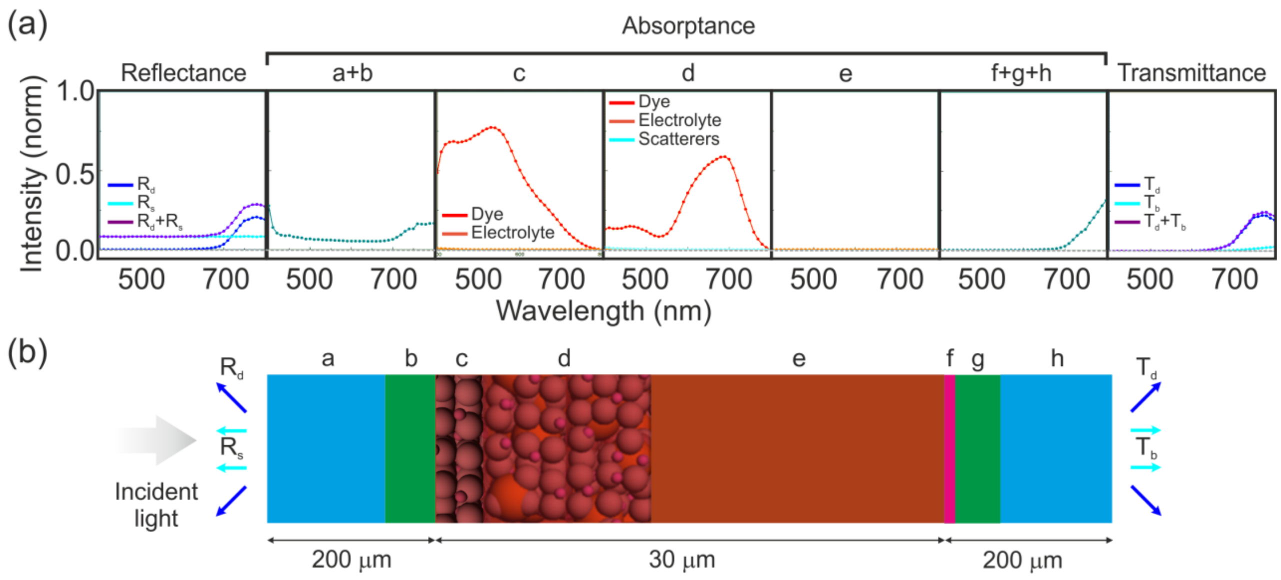

Figure S7. (a) Theoretical results of reflectance (left panel), absorptance (intermediate panels) and transmittance (right panel) for the same optimized system considered in Figure 6 in the main manuscript (a flexible DSC with an structured 12.3 micron electrode consisting on an initial TiO_2 layer without scatterers, followed by an electrode containing 30% TiO_2 particles of r = 160 nm). The cell is illuminated from the PEN substrate as indicated in the schematics (panel (b)). Dashed grey line accounts for reflectance, absorptance or transmittance. Diffuse and specular reflectance are labeled by $R_d(\lambda)$ and $R_s(\lambda)$, respectively, and diffuse and ballistic transmittance by $T_d(\lambda)$ and $T_b(\lambda)$, respectively. Each absorptance panel correspond to each element comprising the cell: [a+b] PEN and ITO substrate, [c] 'adhesion layer' (distinguishing each component, i.e., dye molecules and electrolyte), [d] electrode (distinguishing dye molecules, electrolyte and TiO_2 scatterers), [e] electrolyte, and [f+g+h] counter electrode (platinized PEN/ITO). (b) Schematic of the multilayer DSC containing light scatterers, displaying corresponding slab thicknesses.

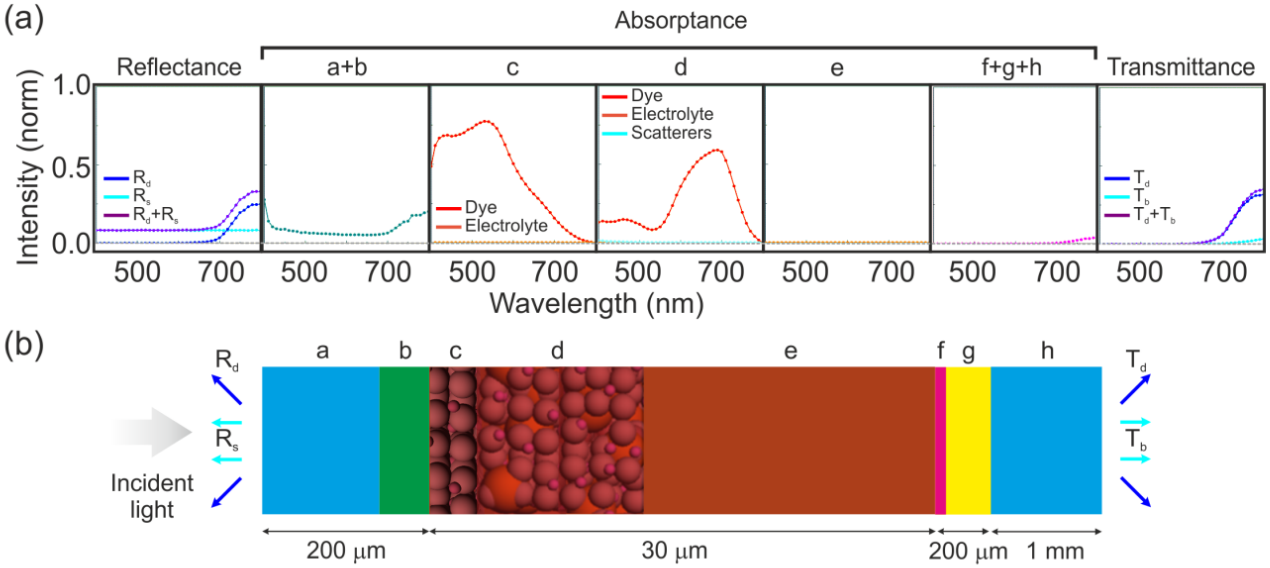

Figure S8. (a) Theoretical results of reflectance (left panel), absorptance (intermediate panels) and transmittance (right panel) for the same optimized system considered in Figure S7 but taking a rigid counter electrode (platinized FTO on glass). The cell is illuminated from the PEN substrate as indicated in the schematics (panel (b)). Dashed grey line accounts for reflectance, absorptance or transmittance. Diffuse and specular reflectance are labeled by $R_d(\lambda)$ and $R_s(\lambda)$, respectively, and diffuse and ballistic transmittance by $T_d(\lambda)$ and $T_b(\lambda)$, respectively. Each absorptance panel correspond to each element comprising the cell: [a+b] PEN and ITO substrate, [c] 'adhesion layer' (distinguishing each component, i.e., dye molecules and electrolyte), [d] electrode (distinguishing dye molecules, electrolyte and TiO_2 scatterers), [e] electrolyte, and [f+g+h] counter electrode (platinized FTO on glass). (b) Schematic of the multilayer DSC containing light scatterers, displaying corresponding slab thicknesses.

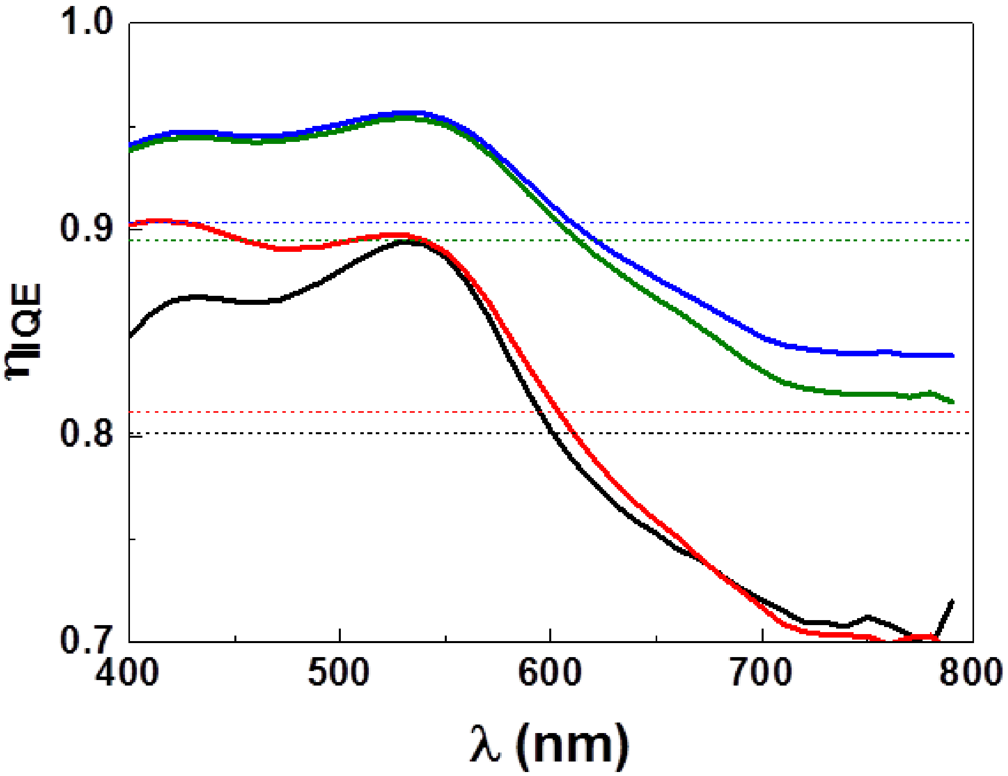

Figure S9. Theoretical calculations of the $\eta_{IQE}(\lambda)$ of all solar cells considered in the main manuscript. Black curve correspond to a plastic cell with a 8.55 micron electrode without scatterers (taking $L_e = 8$ microns); red curve to a plastic cell with a 8.65 micron electrode containing 30% of scatterers of r = 160nm; blue curve to a plastic cell of 11.3 micron electrode (2.8 micron layer without scatterers and a second layer on top with 30% scatterers of r = 160nm); and green curve to a flexible cell of 12.3 micron electrode (2.5 micron layer without scatterers and a 9.8 micron layer on top with 30% scatterers of r = 160 nm).

---

[1] E. Nichelatti, *J. Opt. A: Pure Appl. Opt.* 2002, **4**, 400–403.

[2] R. Santbergen, A.H.M. Smets, and M. Zeman, *Opt. Express* 2013, **21**, S2.

[3] M. Anaya, G. Lozano, M. E. Calvo, W. Zhang, M. B. Johnston, H. J. Snaith and H. Míguez, *J. Phys. Chem. Lett.*, 2015, **6**, 48-53